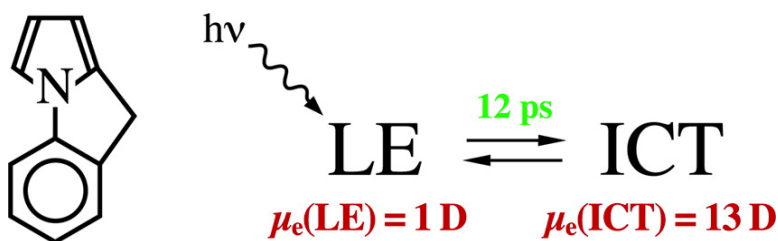


Fast Intramolecular Charge Transfer with a Planar Rigidized Electron Donor/Acceptor Molecule

Toshitada Yoshihara, Sergey I. Druzhinin, and Klaas A. Zachariasse

J. Am. Chem. Soc., **2004**, 126 (27), 8535-8539 • DOI: 10.1021/ja049809s • Publication Date (Web): 18 June 2004

Downloaded from <http://pubs.acs.org> on March 31, 2009



More About This Article

Additional resources and features associated with this article are available within the HTML version:

- Supporting Information
- Links to the 4 articles that cite this article, as of the time of this article download
- Access to high resolution figures
- Links to articles and content related to this article
- Copyright permission to reproduce figures and/or text from this article

[View the Full Text HTML](#)



ACS Publications
 High quality. High impact.

Fast Intramolecular Charge Transfer with a Planar Rigidized Electron Donor/Acceptor Molecule

Toshitada Yoshihara,[†] Sergey I. Druzhinin, and Klaas A. Zachariasse*

Contribution from the Max-Planck-Institut für biophysikalische Chemie, Spektroskopie und Photochemische Kinetik, 37070 Göttingen, Germany

Received January 12, 2004; E-mail: kzachar@gwdg.de

Abstract: The planar rigidized molecule fluorazene (FPP) undergoes fast reversible intramolecular charge transfer (ICT) in the excited state, with a reaction time of 12 ps in the polar solvent ethyl cyanide at -45 °C. The ICT state of FPP has a dipole moment $\mu_e(\text{ICT})$ of 13 D, much larger than that of the locally excited state LE (1 D). The ICT behavior of FPP is similar to that of its flexible counterpart *N*-phenylpyrrole (PP), for which $\mu_e(\text{ICT}) = 12$ D. These results show that intramolecular charge transfer to a planar ICT state can occur efficiently. In designing ICT systems capable of rapid switching, it is therefore important to realize that large amplitude motions such as those necessary for the formation of a twisted intramolecular charge transfer (TICT) state are not required.

Introduction

Electron donor(D)/acceptor(A) molecules such as 4-amino-benzonitriles^{1–3} and *N*-phenylpyrroles,^{1,3–6} can emit fluorescence from two relaxed singlet excited states (dual fluorescence). Upon photoexcitation a locally excited state (LE) is formed, from which an intramolecular charge transfer (ICT) state with a larger dipole moment is produced. With 4-(dimethylamino)benzonitrile (DMABN), for example, the dipole moment increases from 6.6 D in the electronic ground state (μ_g) via 10 D for LE to 17 D for the ICT state ($\mu_e(\text{ICT})$).^{7,8} In the case of *N*-phenylpyrrole (PP), $\mu_g = 1.4$ D and $\mu_e(\text{ICT}) = 12$ D.⁶ Since its discovery around 1960,⁹ dual fluorescence (LE + ICT) has been observed with a large number of D/A molecules in dilute solution,^{1–9} in crystals,¹⁰ and also in the gas phase.¹¹ It is now well-established that this process is an intramolecular phenomenon and that the LE and ICT states are structural conformers.^{1–11}

A controversy still exists, however, concerning the molecular structure of the ICT state.^{12,13} In the twisted intramolecular charge transfer (TICT) model,^{1,3,12} the dimethylamino group of

DMABN, for example, is considered to be twisted to a configuration perpendicular to the plane of the phenyl ring, whereas in the planar intramolecular charge transfer (PICT) model,^{13–15} the dimethylamino and benzonitrile moieties have a largely coplanar structure.

The experiments initially used to support the TICT model were based on compounds having either a rigid planar structure (1-methyl-5-cyanoindoline and 1-methyl-6-cyano-1,2,3,4-tetrahydroquinoline) and only LE emission or with a strongly twisted amino group in the ground state (3,5-dimethyl-4-(dimethylamino)benzonitrile) and only ICT fluorescence.³ Recent experimental evidence in favor of TICT comes from vibrational (infrared and Raman) spectroscopy.^{16,17} In the spectrum of the ICT state of DMABN^{16,17} and *N*-(4-cyanophenyl)pyrrole (PP4C)¹⁶ the frequency attributed to the *N*-phenyl bond stretch is shifted to lower energies by about 160 cm^{-1} relative to that of the ground state. This was considered to be caused by a lengthening of this bond, as predicted by the TICT model (electronic decoupling of the D and A subsystems). In conflict with this interpretation, the quinoidal character of the phenyl ring of the ICT state is larger than that in the ground state, whereas a decrease in quinoidality should occur for a TICT structure.¹⁶ Definite structural conclusions on bond lengths and molecular structure can therefore not be derived from the vibrational spectra of DMABN or PP4C until reliable quantumchemical calculations of the transient spectra are available.¹⁸

[†] Present address: Department of Chemistry, Gunma University, Kiryu, Gunma 376-8515, Japan.

- (1) Rettig, W. *Angew. Chem., Int. Ed. Engl.* **1986**, *25*, 971.
- (2) Demeter, A.; Druzhinin, S.; George, M.; Haselbach, E.; Roulin, J.-L.; Zachariasse, K. A. *Chem. Phys. Lett.* **2000**, *323*, 351.
- (3) Grabowski, Z. R.; Rotkiewicz, K.; Rettig, W. *Chem. Rev.* **2003**, *103*, 3899.
- (4) Rettig, W.; Marschner, F. *New J. Chem.* **1990**, *14*, 819.
- (5) Cornelissen-Gude C.; Rettig, W. *J. Phys. Chem. A* **1998**, *102*, 7754.
- (6) Yoshihara, T.; Galievsky, V. A.; Druzhinin, S. I.; Saha, S.; Zachariasse, K. A. *Photochem. Photobiol. Sci.* **2003**, *2*, 342.
- (7) Schuddeboom, W.; Jonker, S. A.; Warman, J. M.; Leinhos, U.; Kühnle, W.; Zachariasse, K. A. *J. Phys. Chem.* **1992**, *96*, 10809.
- (8) Baumann, W.; Bischof, H.; Fröhling, J.-C.; Brittinger, C.; Rettig, W.; Rotkiewicz, K. *J. Photochem. Photobiol., A* **1992**, *64*, 49.
- (9) Lippert, E.; Lüder, W.; Moll, F.; Nägele, W.; Boos, H.; Prigge, H.; Seibold-Blankenstein, I. *Angew. Chem.* **1961**, *73*, 695.
- (10) Druzhinin, S. I.; Demeter, A.; Zachariasse, K. A. *Chem. Phys. Lett.* **2001**, *347*, 421.
- (11) Daum, R.; Druzhinin, S. I.; Ernst, D.; Rupp, L.; Schroeder, J.; Zachariasse, K. A. *Chem. Phys. Lett.* **2001**, *341*, 272.
- (12) Rettig, W.; Bliss, B.; Dirnberger, K. *Chem. Phys. Lett.* **1999**, *305*, 8.
- (13) Zachariasse, K. A. *Chem. Phys. Lett.* **2000**, *320*, 8.

- (14) Il'ichev, Yu. V.; Kühnle, W.; Zachariasse, K. A. *J. Phys. Chem. A* **1998**, *102*, 5670.
- (15) Zachariasse, K. A.; Grobys, M.; von der Haar, Th.; Hebecker, A.; Il'ichev, Yu. V.; Jiang, Y.-B.; Morawski, O.; Kühnle, W. *J. Photochem. Photobiol., A* **1996**, *102*, 59. Erratum: *J. Photochem. Photobiol., A* **1998**, *115*, 259.
- (16) Okamoto, H.; Inishi, H.; Nakamura, Y.; Kohtani, S.; Nakagaki, R. *J. Phys. Chem. A* **2001**, *105*, 4182.
- (17) Ma, C.; Kwok, W. M.; Matousek, P.; Parker, A. W.; Phillips, D.; Toner, W. T.; Towrie, M. *J. Phys. Chem. A* **2002**, *106*, 3294 and references cited therein.
- (18) Okamoto, H.; Kinoshita, M.; Kohtani, S.; Nakagaki, R.; Zachariasse, K. A. *Bull. Chem. Soc. Jpn.* **2002**, *75*, 957.

A further experiment interpreted as supporting a TICT structure is the syn–anti photoisomerization observed with a cyanopyridine derivative in the protic solvent methanol at low temperature.¹⁹

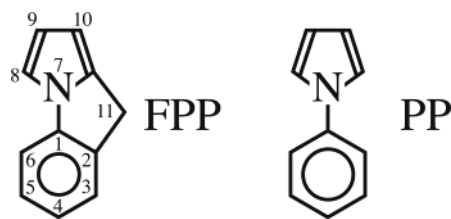
The main arguments in favor of PICT are based on the finding that the amino and benzonitrile parts in the ICT state of a series of 4-(dialkylamino)benzonitriles show a substantial electronic coupling (considered to be absent in a TICT state),¹⁴ as well as from the observation that efficient ICT occurs in planarized 4-aminobenzonitriles with a seven-membered (1-methyl-7-cyano-2,3,4,5-tetrahydro-1*H*-1-benzazepine) or a six-membered (1-*tert*-butyl-6-cyano-1,2,3,4-tetrahydroquinoline, NTC6) alicyclic ring.^{15,20,21} As mentioned above, the absence of dual fluorescence with the 1-methyl and also the 1-ethyl derivative of NTC6 was considered to be one of the main experimental arguments leading to the TICT model.³ Further support for the PICT model comes from picosecond X-ray diffraction measurements with crystalline 4-(diisopropylamino)benzonitrile (DIABN).²² This molecule was chosen because it undergoes efficient ICT in the crystal.¹⁰ The dihedral angle of the amino group relative to the phenyl plane of DIABN was found to be 10° in the ICT state, an effectively coplanar configuration, as compared with 14° in the ground state.²²

In view of these results, it can be concluded that the absence (TICT) or presence (PICT) of electronic coupling between the D and A groups in the ICT state of a D/A molecule, such as that between the phenyl and pyrrole moieties in PP, clearly is a more significant difference between the two ICT models than the presence of an exclusively perpendicular (90°) or coplanar (0°) configuration. In other words, electronic coupling between the D and A subgroups is more important than their twist angle.

Quantumchemical calculations of dual fluorescent D/A molecules such as DMABN and PP, at various levels of sophistication, practically all came to the conclusion that the ICT state has a TICT structure.^{3,23–29} The possibility of a planar ICT state was, however, generally not taken into account. In recent calculations,²⁸ a PICT state was investigated for DMABN, PP, and PP4C, but it was likewise concluded that a TICT state is the most likely molecular structure for the lowest-energy and hence fluorescing ICT state. On the basis of time-dependent density functional theory (TDDFT) calculations with DMABN, it was even concluded that final evidence was provided in favor of the perpendicular twist interpretation and that the TICT–PICT controversy, mainly originating from a discussion of experimental evidence, thereby should become a part of history.²⁹

Here we report on ICT and dual fluorescence observed with fluorazene (FPP; Chart 1), a rigidized planar derivative of PP.

Chart 1



These measurements allow a direct conclusion regarding the structure of the ICT state in these dual fluorescent molecules.

Experimental Section

N-Phenylpyrrole (PP; Chart 1) was purchased from Aldrich. In the synthesis of 9*H*-pyrrolo-[1,2-*a*]-indole (fluorazene, FPP),^{30,31} 1-(2-carboxyphenyl)pyrrole (Maybridge) was reacted with PCl₅ in toluene under addition of SnCl₄. The 9*H*-pyrrolo-[1,2-*a*]-indol-9-one thus obtained was treated with semicarbazide hydrochloride, giving the corresponding semicarbazone, which upon heating to 220–230 °C in diethylene glycol produced fluorazene (mp 88.6–89.6 °C. Literature 89–90 °C (ref 30)). With PP and FPP, HPLC was the last purification step. The identity of FPP was established by NMR and mass spectroscopy. The assignment is based on two-dimensional NMR spectra (HH-COSY, HSQC, HMBC). The ¹H and ¹³C NMR spectra were measured with a Varian Mercury 300 spectrometer. ¹H NMR (300 MHz, CDCl₃, in ppm) for FPP: 3.83 (s, br, CH₂), 7.38 (d, H3), 7.08 (m, H4), 7.27 (m, H5), 7.26 (m, H6), 7.09 (m, H8), 7.08 (t, H9), 6.1 (m, H10). The alkylcyanide solvents acetonitrile (MeCN, Merck, Uvasol), ethyl cyanide (EtCN, Fluka, for analysis), *n*-propyl cyanide (PrCN, Fluka, for analysis), and *n*-butyl cyanide (BuCN, Fluka, pure) were chromatographed over Al₂O₃. The solutions, with an optical density between 0.4 and 0.6 for the maximum of the first band in the absorption spectrum, were deaerated with nitrogen (15 min).

The fluorescence spectra were measured with quantum-corrected Shimadzu RF-5000PC or ISA-SPEX Fluorolog 3-22 spectrofluorometers. Fluorescence quantum yields Φ_f , with an estimated reproducibility of 2%, were determined with quinine sulfate in 1.0 N H₂SO₄ as a standard ($\Phi_f = 0.546$ at 25 °C).³² The fluorescence decay times were obtained with a picosecond laser system (excitation wavelength λ_{exc} : 276 nm) consisting of a mode-locked titanium-sapphire laser (Coherent, MIRA 900F) pumped by an argon ion laser (Coherent, Innova 415) or with a nanosecond (λ_{exc} : 296 nm) flashlamp single-photon counting (SPC) setup. These setups and the procedure used for the analysis of the fluorescence decays have been described previously.^{33,34} The instrument response function of the laser SPC system has a half-width of 18 ps.

Results and Discussion

Fluorescence Spectra. The fluorescence spectrum of FPP in the polar solvent acetonitrile (MeCN) at –45 °C (Figure 1a) consists of two well-separated bands, similar to the LE and ICT emissions of PP (Figure 1b). The two bands are separated by subtraction with the fluorescence spectrum of *N*-(4-methylphenyl)pyrrole (PP4M) adopted as the LE model compound, as PP4M does not undergo an ICT reaction.⁶ Analogous to the ICT/LE fluorescence quantum yield ratio $\Phi'(ICT)/\Phi(LE)$ of PP, the band intensity ratio of FPP becomes smaller with decreasing

- (19) Dobkowski, J.; Wójcik, J.; Koźmiński, W.; Kołos, R.; Waluk, J.; Michl, J. *J. Am. Chem. Soc.* **2002**, *124*, 2406.
 (20) Zachariasse, K. A.; Grobys, M.; von der Haar, Th.; Hebecker, A.; Il'ichev, Yu. V.; Morawski, O.; Rückert, I.; Kühnle, W. *J. Photochem. Photobiol., A* **1997**, *105*, 373.
 (21) Zachariasse, K. A.; Druzhinin, S. I.; Bosch, W.; Machinek, R. *J. Am. Chem. Soc.* **2004**, *126*, 1705.
 (22) Techert, S.; Zachariasse, K. A. *J. Am. Chem. Soc.* **2004**, *126*, 5593.
 (23) Dreyer, J.; Kummrow, A. *J. Am. Chem. Soc.* **2000**, *122*, 2577.
 (24) Parusel, A. B. *J. Phys. Chem. Chem. Phys.* **2000**, *2*, 5545.
 (25) Jamorski Jödicke, C.; Lüthi, H. P. *J. Chem. Phys.* **2002**, *117*, 4146.
 (26) Proppe, B.; Merchán, M.; Serrano-Andrés, L. *J. Phys. Chem. A* **2000**, *104*, 1608.
 (27) Mennucci, B.; Toniolo, A.; Tomasi, J. *J. Am. Chem. Soc.* **2000**, *122*, 10621.
 (28) Zilberg, S.; Haas, Y. *J. Phys. Chem. A* **2002**, *106*, 1.
 (29) Rappoport, D.; Furche, F. *J. Am. Chem. Soc.* **2004**, *126*, 1277.

- (30) Laschtuvka, E.; Huisgen, R. *Chem. Ber.* **1960**, *93*, 81.
 (31) Sydney Bailey, A.; Scott, P. W.; Vandrevalla, M. N. *J. Chem. Soc., Perkin Trans. 2*, **1980**, 97.
 (32) Demas, J. N.; Crosby, G. A. *J. Phys. Chem.* **1971**, *75*, 991.
 (33) Zachariasse, K. A.; Yoshihara, T.; Druzhinin, S. I. *J. Phys. Chem. A* **2002**, *106*, 6325. Erratum: *J. Phys. Chem. A* **2002**, *106*, 8978.
 (34) Il'ichev, Yu. V.; Kühnle, W.; Zachariasse, K. A. *Chem. Phys.* **1996**, *211*, 441.

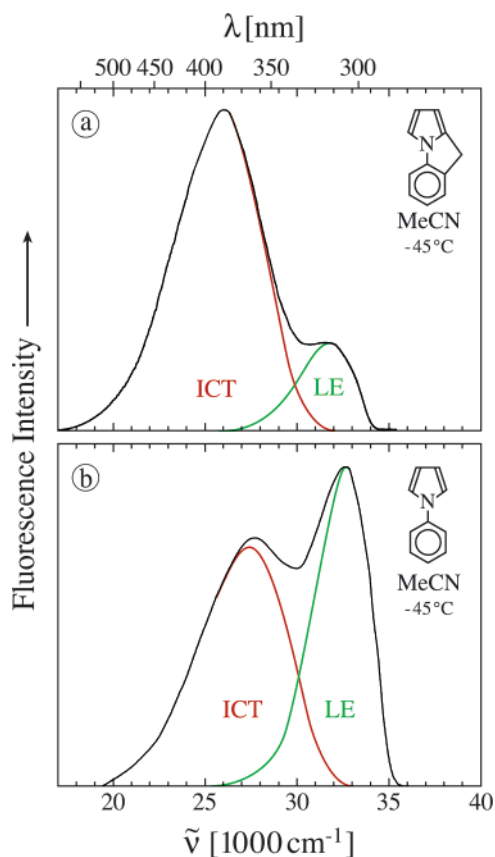


Figure 1. Fluorescence spectra of (a) fluorazene (FPP) and (b) *N*-phenylpyrrole (PP) in acetonitrile (MeCN) at -45 °C. The fluorescence spectra consist of emissions from a locally excited (LE) and an intramolecular charge transfer (ICT) state. The spectral subtraction is carried out by adopting the fluorescence spectrum of *N*-(4-methylphenyl)pyrrole to represent the LE emission. Excitation wavelength: 270 nm.

Table 1. Fluorescence Quantum Yield Ratio $\Phi'(ICT)/\Phi'(LE)$ of FPP and PP in Alkyl Cyanides at -45 °C

	MeCN	EtCN	PrCN	BuCN
ϵ^a	50.2	39.0	35.1	27.7
$\Phi'(ICT)/\Phi'(LE)$ (FPP)	5.48	2.75	0.93	0.59
$\Phi'(ICT)/\Phi'(LE)$ (PP)	1.25	0.35	0.22	0.16

^a Dielectric constant at -45 °C (ref 35).

polarity³⁵ in the solvents MeCN, ethyl cyanide (EtCN), *n*-propyl cyanide (PrCN), and *n*-butyl cyanide (BuCN) at this temperature (Table 1). With FPP, as well as with PP,⁶ only LE emission is observed in the nonpolar *n*-hexane and the slightly polar diethyl ether (Figure 2). These results show that the efficiency of the excited-state reaction of FPP indeed increases when the solvent becomes more polar, as should be the case for an ICT reaction.

$\Phi'(ICT)/\Phi'(LE)$ as a Function of Temperature. Stevens-Ban Plots of FPP and PP in MeCN. To get information on the enthalpy change occurring during the LE \rightarrow ICT reaction, the temperature dependence of the ratio $\Phi'(ICT)/\Phi'(LE)$ was determined for FPP and PP in MeCN (eq 1 and Scheme 1).

$$\Phi'(ICT)/\Phi'(LE) = k'_f/k_f \{k_a/(k_d + 1/\tau'_0)\} \quad (1)$$

(35) Landolt-Börnstein, *Numerical Data and Functional Relationships in Science and Technology, New Series*; Madelung, O., Ed.; Springer: Berlin, 1991; Group IV, Vol. 6.

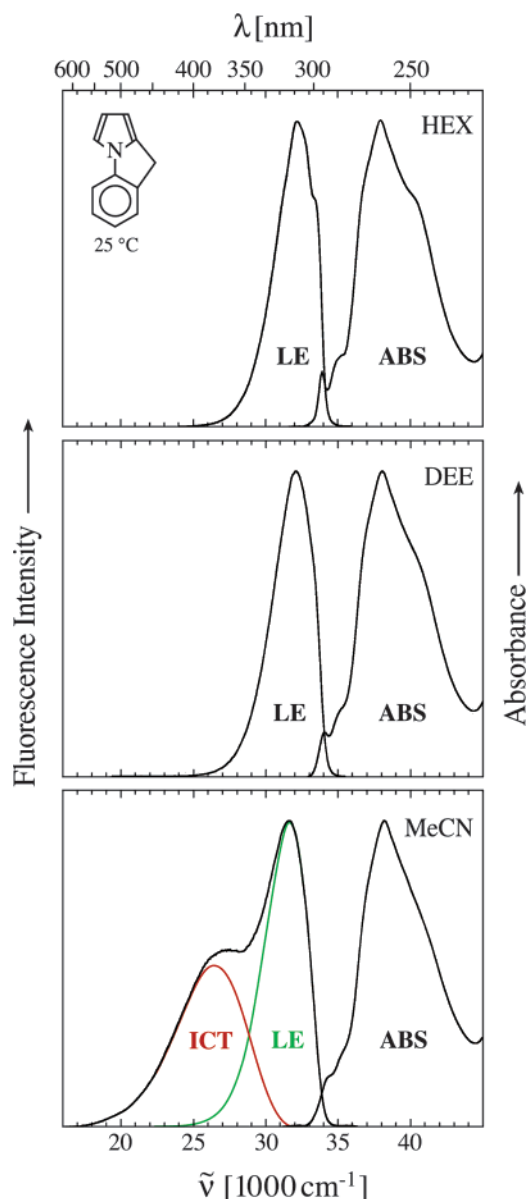
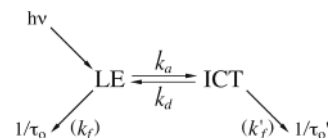


Figure 2. Fluorescence and absorption spectra of FPP in *n*-hexane (HEX), diethyl ether (DEE), and acetonitrile (MeCN) at 25 °C. In *n*-hexane and diethyl ether, the fluorescence spectra consist of an emission from a locally excited (LE) state, whereas in acetonitrile a dual emission from an LE and an intramolecular charge transfer (ICT) state is observed. The spectral subtraction in MeCN is carried out by adopting the fluorescence spectrum of *N*-(4-methylphenyl)pyrrole to represent the LE emission. Excitation wavelength: 270 nm.

Scheme 1



In Scheme 1, k_a and k_d are the rate constants of the forward and backward ICT reaction, $\tau_0(LE)$ and $\tau'_0(ICT)$ are the fluorescence lifetimes, and $k_f(LE)$ and $k'_f(ICT)$ are the radiative rate constants.

From the Stevens-Ban plots in Figure 3, it follows that for both molecules in MeCN the high-temperature limit (HTL, $k_d \gg 1/\tau'_0(ICT)$) holds (Scheme 1) because the data points in these plots do not deviate from the linear HTL dependence.^{36,37} From

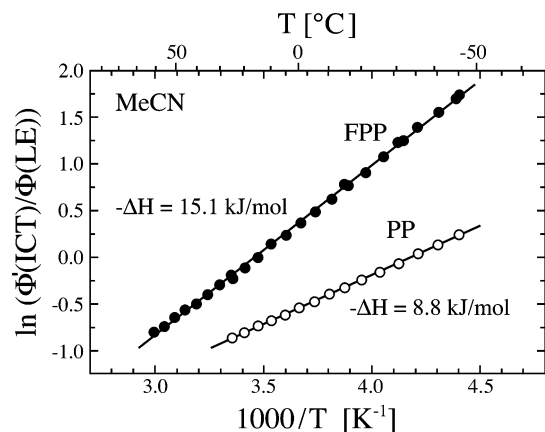


Figure 3. Plots of $\Phi'(ICT)/\Phi(LE)$ versus $1000/T$ for fluorazene (FPP) and *N*-phenylpyrrole (PP) in acetonitrile (MeCN). The value of the change in ΔH for the LE \rightarrow ICT reaction is indicated at the plots.

the slope of the HTL lines in Figure 3, the following values for ΔH in MeCN are calculated: -15.1 kJ/mol for FPP as compared with -8.8 kJ/mol for PP.

ICT and LE Excited-State Dipole Moments. The excited-state dipole moment μ_e of the state emitting the red-shifted additional band of FPP, an indication for the extent of charge separation (ICT) when compared with the ground-state dipole moment μ_g , can be determined by the solvatochromic method from the solvent polarity dependence of the energy of the fluorescence maximum $\tilde{\nu}^{\max}$ (fl) of the new emission band (eqs 2 and 3).^{6,8,34,38}

$$\tilde{\nu}^{\max}(\text{fl}) = -\frac{2}{hc\rho^3} \mu_e(\mu_e - \mu_g)(f(\epsilon) - (1/2)f(n^2)) + \text{constant} \quad (2)$$

where

$$f(\epsilon) - \frac{1}{2}f(n^2) = \frac{(\epsilon - 1)}{(2\epsilon + 1)} - \frac{1}{2} \frac{(n^2 - 1)}{(2n^2 + 1)} \quad (3)$$

In eq 2, ρ is the Onsager radius of the solute, h is the Planck constant, and c is the speed of light, whereas ϵ and n are the dielectric constant and refractive index of the solvent.

By plotting $\tilde{\nu}^{\max}$ (fl) against the solvent polarity parameter $f(\epsilon) - 1/2 f(n^2)$ in Figure 4 (eq 2), a dipole moment μ_e of 13 ± 1 D is calculated. In this procedure, the ground-state dipole moment μ_g (1.7 D) and the Onsager radius ρ (4.15 \AA)⁶ of FPP are employed. The dipole moment μ_g was determined by measuring ϵ and n as a function of FPP concentration.³⁹ On the basis of what has been established for PP,⁶ the dipole moment μ_g is assumed to have a direction opposite to that in the excited state. The radius ρ for FPP was calculated in a manner analogous to the procedure described previously for PP.⁶ The emission maxima $\tilde{\nu}^{\max}$ (fl) of FPP are also plotted against the corresponding maxima⁶ of DMABN and PP4C (Figure 5), resulting in a somewhat smaller dipole moment of 11 D (Table 2). In this manner, the influence of specific solvent interactions as well

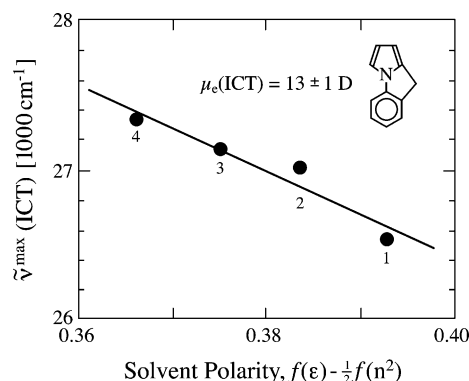


Figure 4. Plot of the ICT emission maxima $\tilde{\nu}^{\max}$ (ICT) of fluorazene (FPP) at 25 °C, against the solvent polarity parameter $f(\epsilon) - 1/2 f(n^2)$ (eq 3). Solvents: (1) acetonitrile, (2) ethyl cyanide, (3) *n*-propyl cyanide, (4) *n*-butyl cyanide.

Table 2. Dipole Moments^a μ_g and μ_e (ICT) (in D) of FPP

	μ_g	μ_e (ICT) ^b	μ_e (ICT) ^c	μ_e (ICT) ^d
FPP	1.7	13 ± 1	11 ± 0.4	11 ± 1

^a The dipole moment μ_e (ICT) has a direction opposite to that in the ground state (μ_g); see text. ^b See Figure 4. ^c See Figure 5a. ^d See Figure 5b.

as the impact of the choice of the magnitude of ρ in the comparison of FPP and PP can be minimized, as has been discussed in detail elsewhere.⁶

From the value of 13 D obtained for the red-shifted fluorescence band of FPP (Figure 4), it follows that this band indeed originates from an ICT state, with a dipole moment slightly larger than that of PP (12 D),⁶ likewise determined from a plot of $\tilde{\nu}^{\max}$ (fl) versus $f(\epsilon) - 1/2 f(n^2)$. For the LE state of FPP, a dipole moment of around 1 D was obtained in a similar manner. These results clearly show that in the rigidized planar molecule FPP, not able to form a perpendicularly twisted TICT state, an efficient excited-state reaction takes place to an ICT state with properties similar to those of its flexible counterpart PP. This is an indication that the ICT state of PP is also planar.

As large amplitude motions are not likely to take place during the ICT reaction of FPP, it is concluded that the structural changes between the LE and ICT state, i.e., the reaction coordinate, mainly involve changes in the bond lengths of PP in these excited states. An example of bond length changes occurring in electron-transfer reactions can be found in the transformation of *N,N,N',N'*-tetramethyl-*p*-phenylenediamine (TMPD) to its radical cation TMPD⁺.^{40,41}

LE and ICT Fluorescence Decays. To investigate the LE and ICT fluorescence dynamics of FPP, time-correlated single-photon counting measurements were made.^{2,10} A global analysis of the LE and ICT fluorescence decays of FPP in EtCN at -45 °C is shown in Figure 6, with common decay times τ_2 and τ_1 (eqs 4 and 5). Two decay times ($\tau_2 = 11$ ps and $\tau_1 = 13.18$ ns) are sufficient to fit the LE decay, whereas only in the ICT decay a minor contribution from an additional time of 32 ps appears, which is attributed to a photochemical degradation product emitting in the same spectral region as the ICT state. The

(36) Leinhos, U.; Kühnle, W.; Zachariasse, K. A. *J. Phys. Chem.* **1991**, *95*, 2013.

(37) Druzhinin, S.; Demeter, A.; Niebuer, M.; Tauer, E.; Zachariasse, K. A. *Res. Chem. Intermed.* **1999**, *25*, 531.

(38) Liptay, W. In *Excited States*; Lim, E. C., Ed.; Academic Press: New York, 1974; Vol. 1, p 129.

(39) Hedestrand, G. *Z. Phys. Chem. B* **1929**, *2*, 428.

(40) Ikemoto, I.; Katagiri, G.; Nishimura, S.; Yakushi, K.; Kuroda, H. *Acta Crystallogr.* **1979**, *B35*, 2264.

(41) De Boer, J. L.; Vos, A. *Acta Crystallogr.* **1972**, *B28*, 835.

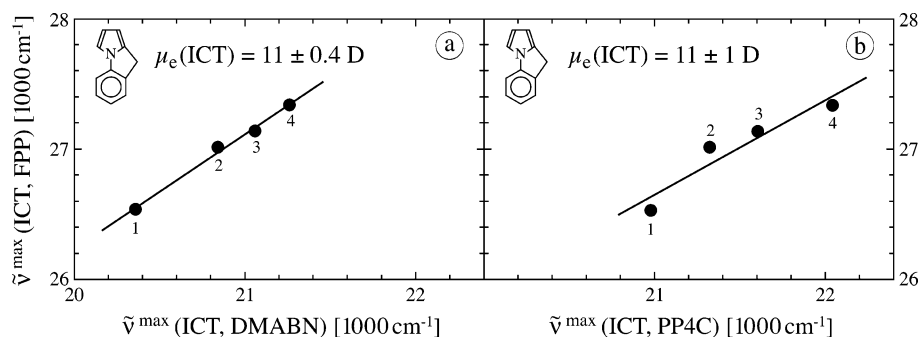


Figure 5. Plot of the ICT emission maxima $\tilde{\nu}^{\max}$ (ICT) of fluorazene (FPP) at 25 °C, against the corresponding $\tilde{\nu}^{\max}$ (ICT) data of 4-(dimethylamino)-benzonitrile (DMABN) and of *N*-(4-cyanophenyl)phenylpyrrole (PP4C) (eq 2). Solvents: (1) acetonitrile, (2) ethyl cyanide, (3) *n*-propyl cyanide, (4) *n*-butyl cyanide.

Table 3. Decay and ICT Parameters of FPP and PP in Ethyl Cyanide at -45 °C (eqs 4 and 5 and Scheme 1)

	τ_2 (ns)	τ_1 (ns)	A_{12}/A_{11}	τ_0 (ns)	k_a (10^{10} s^{-1})	k_d (10^{10} s^{-1})	τ'_0 (ns)	ΔG^\ddagger (kJ/mol)
FPP	0.011	13.18	9.03	11.7	8.2 ± 0.7	0.9 ± 0.1	13.4	-4.2 ± 0.3
PP	0.016	6.52	1.35	11.7	3.7 ± 0.8	2.7 ± 0.3	4.9	-0.6 ± 0.4

^a From $\Delta G = -RT \ln(k_a/k_d)$. The standard deviations of k_a , k_d , and ΔG were calculated by adopting a reproducibility error of 1 ps for τ_2 , 50 ps for τ_0 and τ_1 , and 10% for A .

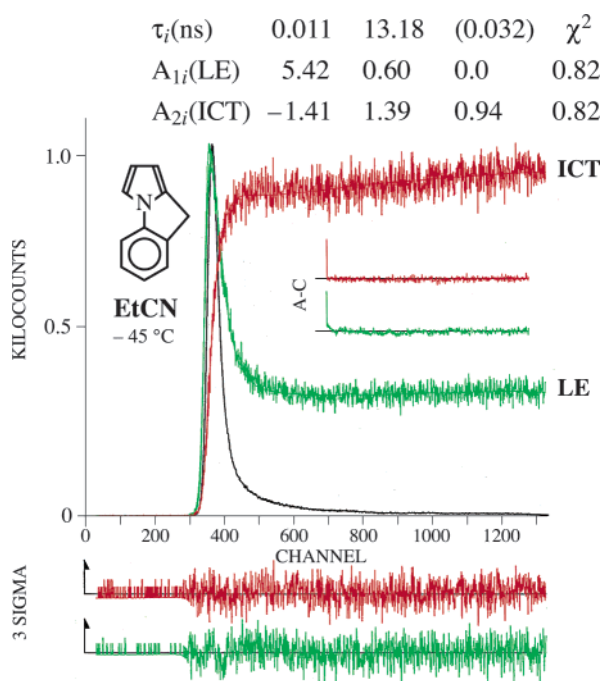


Figure 6. LE and ICT fluorescence response functions of FPP in ethyl cyanide (EtCN) at -45 °C. The LE and ICT decays are analyzed simultaneously (global analysis). The decay times (τ_1, τ_2) and their preexponential factors A_{1i} and A_{2i} are given (eqs 4 and 5). The shortest decay time τ_2 is listed first. The time in parentheses, only present as a minor contribution in the ICT decay, is attributed to a photoproduct (see text). The weighted deviations, expressed in σ (expected deviations), the auto-correlation functions A–C, and the values for χ^2 are also indicated. Excitation wavelength: 279 nm. Emission wavelengths: 310 nm (LE), 430 nm (ICT).

presence of a negative amplitude for the shortest ICT decay time τ_2 with an amplitude ratio A_{22}/A_{21} close to -1 (eq 5) indicates that the ICT state of FPP cannot be formed by direct

excitation of the ground state, similar to what has been observed with DMABN and related molecules.^{14,36}

$$i_f(\text{LE}) = A_{11} \exp(-t/\tau_1) + A_{12} \exp(-t/\tau_2) \quad (4)$$

$$i_f(\text{ICT}) = A_{21} \exp(-t/\tau_1) + A_{22} \exp(-t/\tau_2) \quad (5)$$

This decay analysis of FPP corresponds to that for a two-state model (Scheme 1) consisting of an LE state from which an ICT state is formed after photoexcitation.

From the decay times τ_1 , τ_2 , and the amplitude ratio A_{12}/A_{11} ($= 9.03$) of the LE decay of FPP in EtCN at -45 °C in Figure 6 (eq 4), together with the lifetime τ_0 (11.7 ns) of the LE model compound PP4M,⁶ the ICT rate constants k_a and k_d and the lifetime τ'_0 of the ICT state can be determined.^{14,36} The results are: $k_a = 8.2 \times 10^{10} \text{ s}^{-1}$, $k_d = 0.9 \times 10^{10} \text{ s}^{-1}$, and $\tau'_0(\text{ICT}) = 13.4 \text{ ns}$ (Table 3). For PP, the following data were obtained: $k_a = 3.7 \times 10^{10} \text{ s}^{-1}$, $k_d = 2.7 \times 10^{10} \text{ s}^{-1}$, and $\tau'_0 = 4.9 \text{ ns}$ (Table 3). It is seen from these data that in the planarized molecule FPP the ICT reaction rate constant k_a has become faster than that of PP by a factor of 2. The ICT efficiency can be controlled by changing the solvent polarity and temperature.

Conclusions

With the rigidized planar D/A molecule FPP, efficient ICT occurs in a few picoseconds, without the involvement of large amplitude motions. This means that fast and efficient ICT is possible in planar D/A molecules, showing that perpendicular twisting (TICT) of the D and A moieties is not required in this process. The photophysical similarity of FPP and PP indicates that a TICT state also does not play a role with PP.

Acknowledgment. Many thanks are due to Mr. Wilfried Bosch for the synthesis of FPP. We are grateful to Mr. R. Machinek, Göttingen University, for the analysis and measurement of the NMR spectra.

JA049809S